EVALUATING THE EFFECT OF THE OBSERVATION TIME ON THE DISTRIBUTION OF SAR PERMANENT SCATTERERS

Alessandro Ferretti[(1)], Carlo Colesanti[(2)] , Daniele Perissin[(2)] , Claudio Prati[(2)] , and Fabio Rocca[(2)]

[(1)] Tele-Rilevamento Europa -T.R.E. S.r.l., Via Vittoria Colonna 7, 20149 Milano, Italy – af@treuropa.com
[(2)] Politecnico di Milano, Piazza Leonardo da Vinci 32, 20133 Milano, Italy- rocca@elet.polimi.it

ABSTRACT

This paper deals with the problem of temporal decorrelation in the application of Differential SAR Interferometry (DInSAR) to surface deformation monitoring. Special attention has been paid to the impact of reflectivity changes on the so-called Permanent Scatterers (PS). Semi-PS (SPS) and Temporary PS (TPS) are first defined and possible solutions to their detection are then proposed. The impact of the temporal baseline and satellite repeat-cycle is then discussed based on the analysis of two ERS data-sets of 26 scenes each acquired over Rome. The first one is characterized by a 3-day repeat cycle (Second Ice Phase 1993-1994) and the second spans a 5-year temporal window (1995-2000, 35-day repeat cycle) mimicking the normal baseline distribution of the former. Preliminary results obtained by applying the PS technique to the 3-day repeat cycle data-set shows a much higher PS density than the usual figures obtained with a monthly acquisition scheme, and the possibility to get many measurement points over agricultural fields. The velocity field shows a peculiar behaviour still to be investigated.

1. INTRODUCTION

DInSAR applications have been lately received further momentum by the introduction of new multi-interferogram approaches [1-6]. After the introduction of the Permanent Scatterers (PS) technique [1-3], significant resources have been spent at POLIMI and TRE to study, characterize and possibly overcome its limitations. One of the major concerns was related to the possibility to loose information whenever point scatterers behave as coherent targets only on a limited number of images, i.e. on a sub-set of SAR scenes acquired over the area of interest. In the standard PS analysis, only radar targets coherent over the whole time series of observation can be detected. In the following section, a possible solution to identify PS with a limited lifetime is proposed.
The research of PS with limited lifetime is strongly related to the study of temporal decorrelation phenomena [7], i.e. the change of the reflectivity values of the radar scene. The analysis of two SAR data-sets acquired over the same area, characterized by two different repeat-cycles, is important to get a better understanding of this kind of phenomena and to study the impact of satellite repeat-cycle on PS analysis (a key-issue also for future SAR missions). The analysis of the coherence histograms of many interferograms with different temporal and geometrical baseline forms the background for the comparison and the analysis of PS results. Whenever coherent targets can be identified over agricultural fields and, in general, over non-urban areas (and this turns out to be possible - not only over rocky areas – when short repeat-cycles are available), the analysis of their time series can represent a valuable tool to infer relevant geophysical information. In this paper, we show the very first result of a full PS analysis carried out on 26 ERS-1 acquisitions during the second ice phase.

2. SEMI AND TEMPORARY PS

Following the PS approach, given N SAR images characterized by the same acquisition geometry, we can generate $N-1$ differential interferograms all relative to the same master image. Let T be the temporal baseline value of the generic interferogram. We define SPS (Semi Permanent Scatterer) a radar target that behaves as PS only for interferograms with $T<T_0$ or $T>T_0$. In general, a TPS (Temporary Permanent Scatterer) is a radar target that acts as a PS only for a limited time-period, i.e. a sub-set of interferograms with $T>T_1$ and $T<T_2$. The detection (and exploitation) of SPS and TPS is not an easy task to perform. In fact, even when interferograms have been already compensated for the atmospheric phase components, the joint estimation of both elevation and displacement time series (the key-step in the PS analysis) can not be carried out for all possible values of T_0 or T_1 and T_2. Indeed, the computational burden related to the processing of each image pixel would be huge even with limited data-sets.
The solution we propose is based on the following observations:

- Abrupt changes in the time series of the phase values usually correspond to changes in the amplitude values.
- The higher the amplitude (i.e. the RCS of the target), the higher the probability that the target behaves as PS.
- Fast and reliable algorithms are available to estimate the location of changepoints [8] in gaussian time series.

The first point is reasonable: it seems at least unlikely that an image pixel can suffer a severe change of behaviour of the reflectivity phase with no significant variation of the backscattered energy. The second point is still the subject of an in depth statistical analysis based on more than 4,000 ERS scenes already processed at TRE, aimed at characterizing the ERS PS. However, the results we got so far show a neat relationship between the multi-image reflectivity map (i.e. the

Proc. of FRINGE 2003 Workshop, Frascati, Italy,
1 – 5 December 2003 (ESA SP-550, June 2004) 42_ferrett

incoherent average of the available images) and the probability that a pixel is a PS. In Fig.1 the percentage of pixels that behave as PS for different amplitude values is reported for a data-set of 92 SAR images acquired over Milano. The image power has been normalized to one. In general, whenever the backscattered energy of the target is 12 dB higher than the mean value, the probability is greater than 0.5.

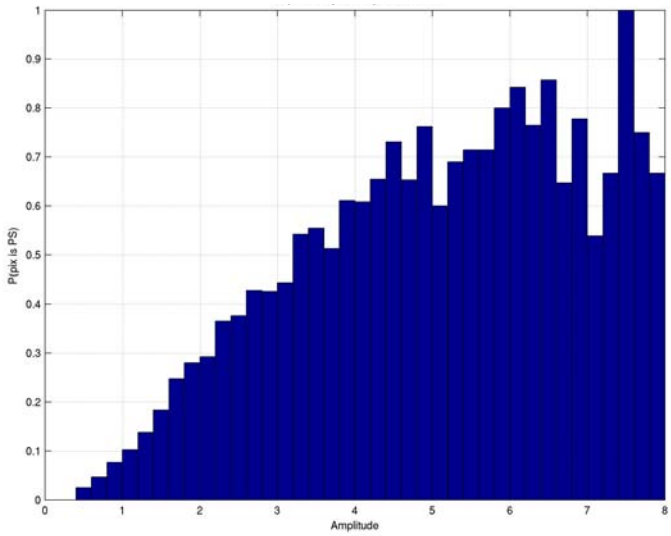

Fig. 1. PS probability vs. amplitude (incoherent average of all available scenes). Milano data-set. 92 images.

The estimation of the value of T_0 or T_1 and T_2 can be estimated from the time series analysis of the amplitude data of the targets. Change-point detection algorithms can be applied successfully. In order to detect SPS, for example, we can apply a Bayesian step detector [8] on the time series of the image pixels. Whenever an abrupt change in the amplitude values is detected, the sub-set of images characterized by higher backscattered energy are processed by means of the PS algorithm. If we consider a gaussian approximation for the statistics amplitude returns (a valid approximation at least when targets behave as PS [1]), fast and efficient algorithms exist. An example is reported in Fig.2.

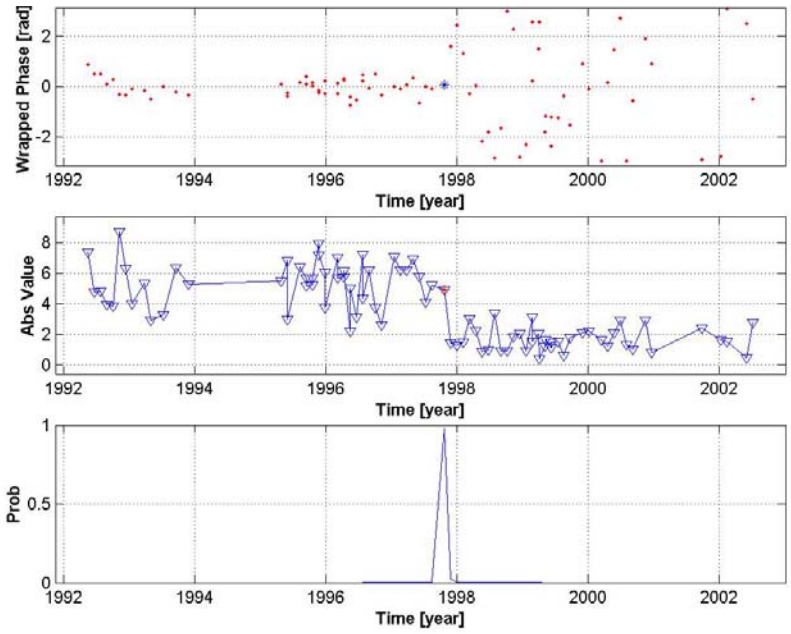

Fig. 2. Example of SPS detection: (a) Time series of the phase values; (b) time series of the amplitude values; (c) change-point probability estimated by the Bayesian step detector considering Gaussian statistics.

In order to detect and measure TPS we extend the step-detector approach to two change-points. TPS detection is far more computational demanding than SPS detection, though the algorithm is still robust and reliable (at least when the number of images is >40 and the target stays coherent for at least 15-20 acquisitions). In general, one should apply this kind of analysis only if it is worth, i.e. when it is mandatory to maximize the information extracted from the data-set.

Preliminary results over urban areas show that the number of SPS is usually 10% of the number of PS on a typical ESA-ERS data-set (1992-2003), while just 1 TPS is found every 100 PS.

3. TEMPORAL DECORRELATION ANALYSIS

Apart from abrupt changes of the reflectivity values of individual scattering centres, temporal decorrelation effects can be due to physical changes in the surface over the time period between the observations: this is the typical scenario in non-urban areas (e.g. vegetated areas and agricultural fields). To study the impact of temporal decorrelation over rural areas two independent ERS data-sets have been processed (3-day repeat cycle: 26 images, Track 22 - Frame 2673. 35-day repeat cycle: 26 images, Track 79 - Frame 2673) characterized by two different repeat cycles but a very similar normal baseline distribution. In fact, images from track 79 have been carefully selected to mimic the 3-day data-set (apart from the temporal baselines). Both data-sets have been acquired over the area of Rome and Colli Albani.
We first computed more then 180 coherence maps and their histograms (Fig.3). The analysis of these data showed a rather abrupt change of shape when the temporal baseline exceeds one month.

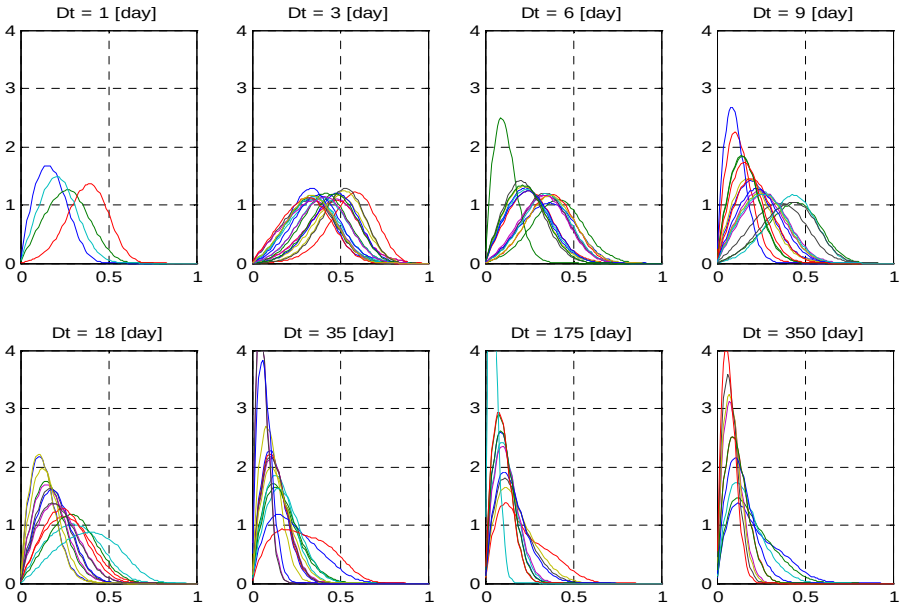

Fig. 3. Coherence histograms for 8 groups of interferograms with different temporal baselines.

The analysis of the behaviour of the coherence values as a function of the temporal (T) and geometrical (B) baseline is interesting and will deserve further research efforts. Preliminary results show that coherence values relative to many target areas can be approximated by applying the following simple model (see for example [7]):

$$\rho_{total} = \rho_{temporal} \cdot \rho_{spatial} \cdot \rho_{thermal\&processing} \approx \max\left\{W, \exp\left\{-\frac{T}{\tau}\right\} \cdot \left(1 - \frac{B}{B_{eff}}\right) \cdot C\right\} \qquad (1)$$

where W and C are numerical parameters (to be estimated) common to all image pixels. W is a bias term dependent on the number of effective looks used for coherence estimation (~45 in our experiment) and C takes into account both thermal noise and processing artefacts. On the contrary, τ and B_{eff} depends on the area under study. Indeed, though B_{eff} should be equal to the so-called critical baseline (about 1100 m for ERS), volumetric effects have to be considered. Typically, the coherence goes to zero at a baseline B_h, if the scatter is uniformly distributed in the altitude of ambiguity h correspondent to that baseline, $h \approx 9000/ B_h$ meters for ERS. In our model, since we have to combine the two effects, we consider an *effective critical baseline*:

$$\rho_{spatial} = \left(1 - \frac{B}{B_{cr}}\right)\left(1 - \frac{B}{B_h}\right) \approx \left(1 - \frac{B}{B_{eff}}\right); \quad \frac{1}{B_{eff}} = \frac{1}{B_{cr}} + \frac{1}{B_h} \qquad (2)$$

As far as the temporal decorrelation is concerned, it is important to highlight how the exponential behaviour with time is consistent with a Brownian motion of the surface. The variance of the surface position would then increase linearly with time and since the coherence is exponentially decreasing with the variance of the surface motion, we get the exponential decay that is approximately measured (see also [7]):

$$\rho_{temporal} = \exp\left\{-\frac{1}{2}\left(\frac{4\pi}{\lambda}\right)^2 \sigma^2_{motion}\right\} \qquad (3)$$

$$\sigma^2_{motion} = \sigma^2_{day} \cdot T$$

where σ^2_{motion} is the variance of the motion component along the LOS, T is the temporal baseline in days. Hence we have:

$$\tau = \frac{\lambda^2}{8 \cdot \sigma^2_{day} \cdot \pi^2} \qquad (4)$$

Over many target areas, we estimated values ranging from 10 to 40 days, corresponding to:

$$\sigma_{day} = 1 \div 2mm \qquad (5)$$

interesting figures that will deserve further analyses. In Fig. 4, an example of fitting of the coherence values is reported.

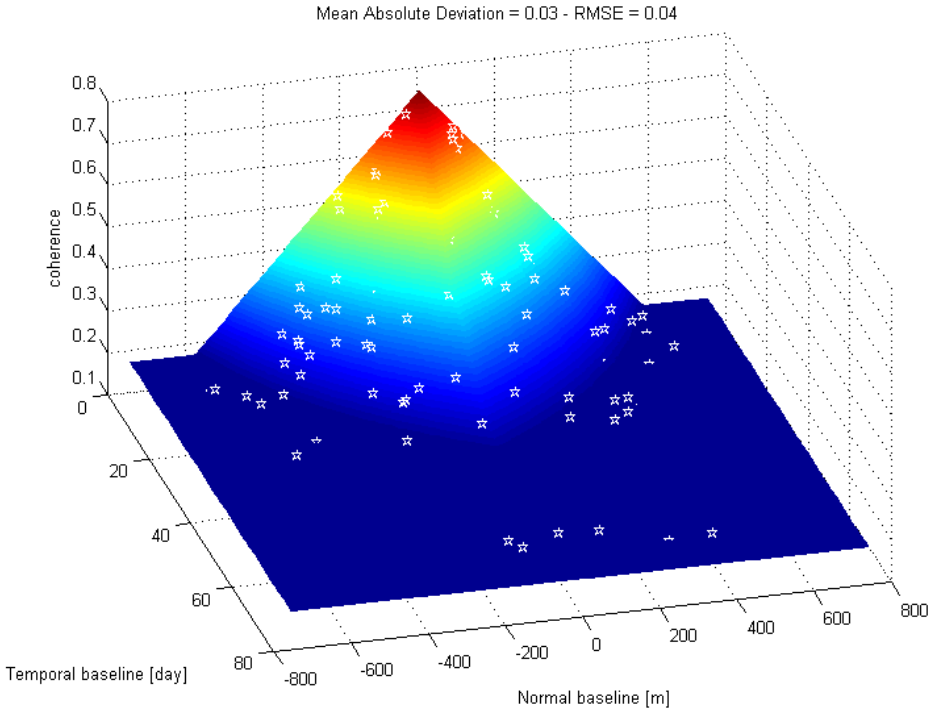

Fig.4. Fitting of coherence values by mean of equation (1). B_{eff}=780 [m] – τ=27 [day].

4. PS ANALYSIS ON 3-DAY AND 35-DAY REPEAT CYCLE DATA STACKS

Two full PS analyses [1-3] were carried out on the two ERS data-sets. As already mentioned in the previous sections, the 26 images of the 35-day repeat-cycle data-set (1995-2000, hereafter "DS35") were carefully selected to resemble the normal baseline dispersion of the 1993-94 data-set (December 1993-April 1994, hereafter "DS3"), trying to highlight the impact of repeat-cycle and temporal baseline values only. For comparison purposes, we tried to use exactly the same processing chain with the same input parameters. After the analysis of the coherence maps, we expected a very different PS density in the two data-sets, mostly due to the shorter repeat-cycle and the low temporal decorrelation.

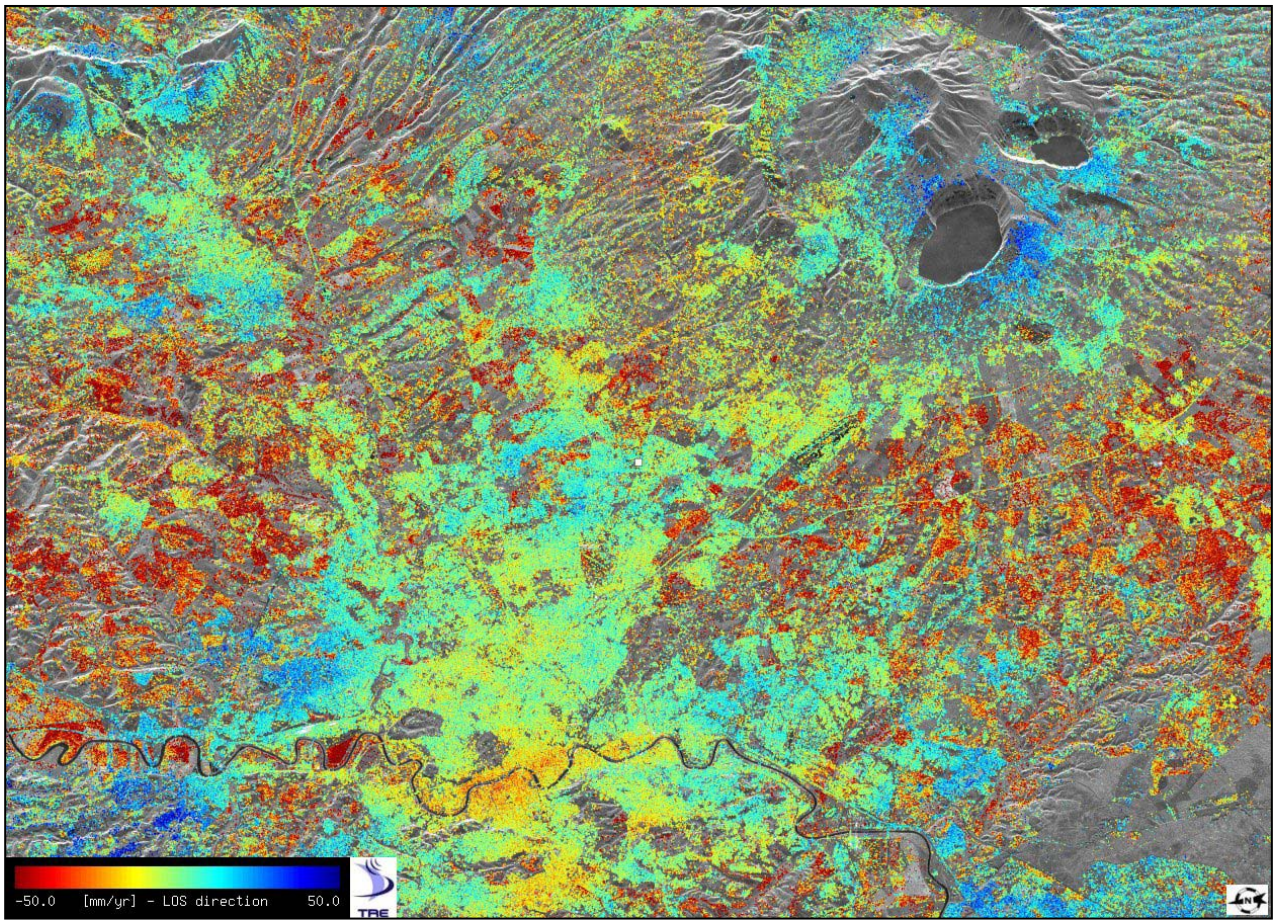

Fig.5. LOS velocity field [mm/yr] estimated from the 3-day repeat cycle data-set (DS3).

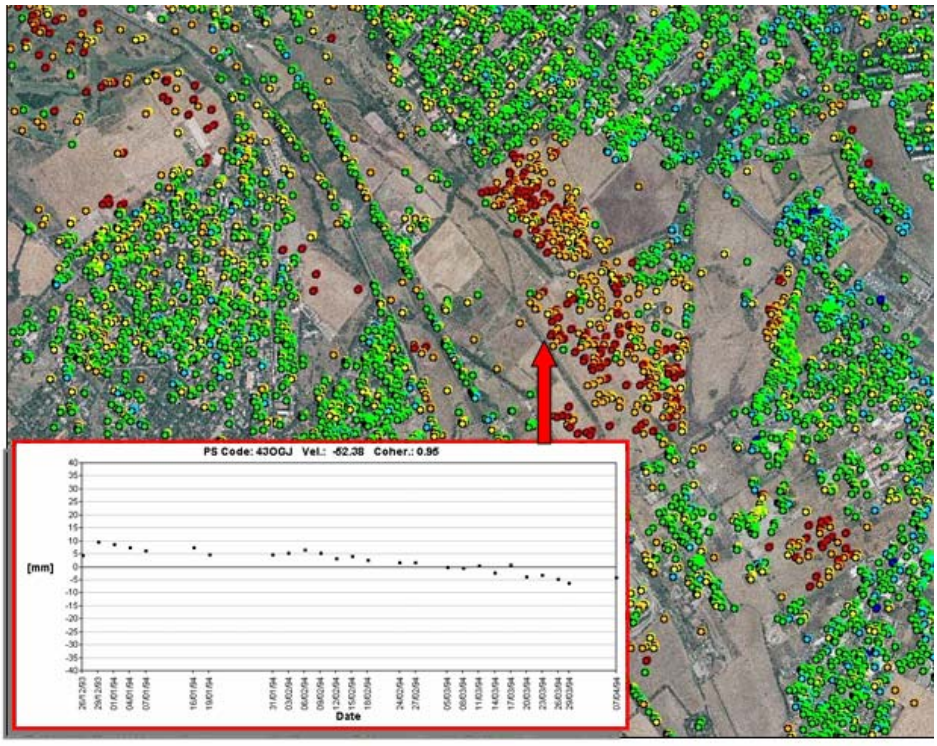

Fig.6. PS (3-day repeat cycle data-set – DS3) superimposed on an aerial photo of a test area. PS affected by significant velocity values do not correspond to buildings or any other man-made structure. On the contrary, they are usually located within agricultural fields.

A thorough analysis of the results is still in progress, the main points are the following:

- During the statistical analysis of the amplitude values (for PS Candidates selection [1]) we found 90,000 targets in DS3 having an amplitude stability index (i.e. the ratio of the mean and the standard deviation) greater than 5. Only 30,000 were identified in DS35.
- 60,000 PS having a phase coherence value greater than 0.9 were identified in DS35. More than 300,000 in DS3 (more than 5 times the PS density typical of non-urban areas in DS35).
- Most of the new PS were identified over rural areas and agricultural fields.
- The LOS velocity field estimated from DS3 (Fig. 5) is intriguing and seems to be related to geophysical signals. Abrupt changes in velocity values correspond to edges of farm fields (Fig. 6).
- Many PS identified over agricultural fields seem to be affected by subsidence rates >50 mm/yr, corresponding to ~12 mm LOS displacement of the electromagnetic centre (Fig. 6).

5. CONCLUSIONS

The standard PS analysis can be improved adding *ad hoc* software algorithms for SPS and TPS detection. The comparison between DS3 and DS35 clearly shows how important could be the adoption of shorter repeat cycle acquisition policies in future SAR constellations. Preliminary results of PS analysis in DS3 show many measurement points over non-urban areas and agricultural fields affected by significant LOS displacement. Prior researches [9-11] suggest that phase variations can be related to irrigation of farm fields and that changes in penetration depth and clay swelling (soil moisture related phenomena), can affect SAR interferograms. At C-band, the typical range of path length variation due to soil moisture change should be less than 20 mm [10], we notice a lowering of the electromagnetic centre of 10-15 mm in about 4 months passing from winter 1993 to spring 1994 (higher mean temperatures). Future research efforts will be devoted to the study of the correlation of the PS results with local soil maps and meteorological information.

6. ACKNOWLEDGEMENTS

The authors wish to thank Jacopo Allievi, Fabrizio Novali as well as the whole TRE technical staff for the PS processing of the data-sets and the development of the software procedures used in this paper. Dr. Ferretti wishes to thank Dr. Matt Nolan of University of Alaska Fairbanks for interesting discussions that further stimulated the PS analysis of short repeat cycle data-sets. This research has been self-financed by TRE and Politecnico di Milano.

7. REFERENCES

1. Ferretti A., Prati C., Rocca F., "Permanent Scatterers in SAR Interferometry" - *IEEE Trans. on Geoscience and Remote Sensing*, Vol. 39, no. 1, January 2001, pp.8-20.
2. Ferretti A., Prati C., Rocca F., "Non-linear Subsidence Rate Estimation Using Permanent Scatterers in Differential SAR Interferometry" – *IEEE Trans. on Geoscience and Remote Sensing,* Vol. 38, no. 5, September 2000, pp.2202-2212.
3. C. Colesanti, A. Ferretti, F. Novali, C. Prati, F. Rocca, "SAR Monitoring of Progressive and Seasonal Ground Deformation Using the Permanent Scatterers Technique", *IEEE Trans. on Geoscience and Remote Sensing,* Vol. 41, no. 7, July 2003, pp.1685-1701.
4. Mora, O.; Mallorqui, J.J.; Broquetas, A. "Linear and nonlinear terrain deformation maps from a reduced set of interferometric SAR images", ", *IEEE Trans. on Geoscience and Remote Sensing,* Vol. 41, no. 10, October 2003, pp. 2243 -2253.
5. P. Berardino, G. Fornaro, R. Lanari, E. Sansosti: "A new Algorithm for Surface Deformation Monitoring based on Small Baseline Differential SAR Interferograms", *IEEE Transactions on Geoscience and Remote Sensing,* Vol. 40, No. 11, November 2002, pp. 2375-2383.
6. Sandwell D. and Price E., "Phase Gradient Approach to Stacking Interferograms"**,** *Journal of Geophysical Research*, v. 103, p. 30183-30204, 1998.
7. Zebker H. and Villasenor, J., "Decorrelation in interferometric radar echoes", *IEEE Trans. on Geoscience and Remote Sensing,* Vol. 30, no. 5, September 1992, pp.950-959.
8. O Ruanaidh J.J.K. and Fitzgerald W.J., *Numerical Bayesian Methods Apllied to Signal Processing*, Springer-Verlag New York, 1996.
9. Gabriel A.K., Goldstein R., and Zebker H.A., "Mapping small elevation changes over large areas: Differential radar interferometry", *Journal of Geophysical Research*, v. 94, p. 9183-9191, 1989.
10. Nolal M. and Fatland D.R., "Penetration Depth as DInSAR Observable and Proxy for Soil Moisture", *IEEE Trans. on Geoscience and Remote Sensing,* Vol. 41, no. 3, March 2003, pp. 532-537.
11. Nolal M., Fatland D.R. and Hinzman L., "DInSAR Measurement of Soil Moisture", *IEEE Trans. on Geoscience and Remote Sensing,* Vol. 41, no. 12, December 2003, *in press*.